Nonlinear dynamics of a cracked cantilever beam under harmonic excitation

Ugo Andreaus, Paolo Casini, Fabrizio Vestroni

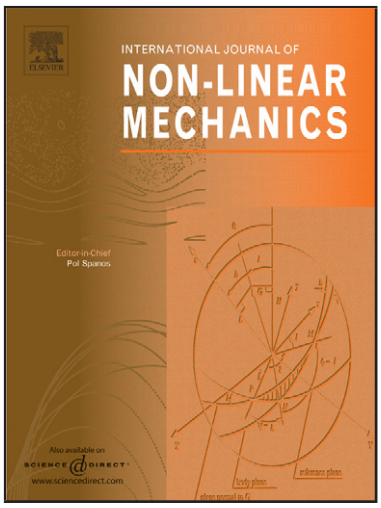

Nonlinear dynamics of a cracked cantilever beam under harmonic excitation

Ugo Andreaus, Paolo Casini, Fabrizio Vestroni

PII: S0020-7462(07)00082-0
DOI: doi:10.1016/j.ijnonlinmec.2006.08.007
Reference: NLM 1357

To appear in: *International Journal of Non-Linear Mechanics*

www.elsevier.com/locate/nlm

Received date: 7 April 2005
Revised date: 26 July 2006
Accepted date: 10 August 2006

Cite this article as: Ugo Andreaus, Paolo Casini and Fabrizio Vestroni, Nonlinear dynamics of a cracked cantilever beam under harmonic excitation, *International Journal of Non-Linear Mechanics* (2007), doi:10.1016/j.ijnonlinmec.2006.08.007

Nonlinear Dynamics of a Cracked Cantilever Beam Under Harmonic Excitation

Ugo Andreaus(*), Paolo Casini(+) and Fabrizio Vestroni(*)

(*) Dipartimento d'Ingegneria Strutturale & Geotecnica

Università degli Studi di Roma "La Sapienza", Via Eudossiana 18 – 00184 Roma, Italy

(+) Dipartimento di Progettazione, Riabilitazione e Controllo delle Strutture Architettoniche,

Università degli Studi di Chieti-Pescara "G. D'Annunzio", Viale Pindaro 42 – 65127 Pescara, Italy

Ph.: 0039-06-44585297; *Fax*: 0039-06-4884852; *E-mail*: ugo.andreaus@uniroma1.it

Abstract

The presence of cracks in a structure is usually detected by adopting a linear approach through the monitoring of changes in its dynamic response features, such as natural frequencies and mode shapes. But these linear vibration procedures do not always come up to practical results because of their inherently low sensitivity to defects. Since a crack introduces nonlinearities in the system, their use in damage detection merits to be investigated. With this aim the present paper is devoted to analyze the peculiar features of the nonlinear response of a cracked beam.

The problem of a cantilever beam with an asymmetric edge crack subjected to a harmonic forcing at the tip is considered as a plane problem and is solved by using two-dimensional finite elements; the behaviour of the breathing crack is simulated as a frictionless contact problem. The modification of the response with respect to the linear one is outlined: in particular, excitation of sub- and super-harmonics, period doubling, quasi-impulsive behaviour at crack interfaces are the main achievements. These response characteristics, strictly due to the presence of a crack, can be used in nonlinear techniques of crack identification.

Keywords: cracked beam, breathing crack, nonlinear forced response, period doubling, quasi-impulsive behaviour.

1. Introduction

The vibration characteristics of cracked structures can be useful for an on-line detection of cracks (non-destructive testing) without actually dismantling the structure. Thus, the development of structural integrity monitoring techniques is received increasing attention in recent years [1,2]. Among these techniques, it is believed that the monitoring of the global dynamics of a structure offers favourable alternative if the on-line (in service) damage detection is necessary. In order to identify structural damage by vibration monitoring, the study of the changes of the structural dynamic behaviour due to cracks is required for developing the detection criterion.

With the ever increasing sophistication of available equipment more effective models had to be built to better interpret the experimental results. In the development of some theoretical models, it has been assumed that the crack remains open [3]. Unfortunately, relying on the drop in the natural frequencies only and using the open crack model could lead to underestimating the severity of the crack [4]. Furthermore, as it has been shown that the modal frequencies are not very sensitive to the presence of a breathing crack, alternative detection techniques have been proposed [5]. They are based upon the analysis of the dynamic nonlinear effects of the crack; in fact they are not exhibited by the intact beam response in the frequency domain, which instead contains only the natural frequencies and the excitation frequency. Chu and Shen [6] made an analogy between cracked beam and a bilinear spring-mass system; their method centred on forcing the beam at a low frequency and observing the resultant spectra. They noted some nonlinear features of the spectra; they in fact observed a modest crack signature from a crack halfway through the thickness of a simply supported beam. More recently, researchers have been looking at the steady state response of the beam to a single harmonic input while including the non linear effects of crack closure and outlining procedures of sub- and super-resonant diagnostics [7].

In summary, the main problem with crack detection methods based on linear vibration analysis has been a lack of sensitivity to the presence of small cracks. This paper is concerned with the possibility of crack detection by exploiting one or more characteristic features of bilinear systems, e. g. the presence of sub- and super-harmonic components in the steady state response of the system. In fact the presence of side peaks in the Fourier spectra may be used as a feature to recognize the presence of fatigue cracks [5].

An asymmetrically cracked beam vibrating in bending will have a bilinear stiffness depending whether the crack is open or closed. In addition, typically the faces of the crack, or clearance, will have nonzero relative velocity on closure, leading to an impulsive effect. From this point of view, few response analyses of cracked structures have taken into account the effect of the alternation of crack opening and closure [8-10].

Aim of this paper is to identify the distinguishing features of the dynamic response associated with the existence of a fatigue crack. The simplest of excitations - that of sinusoidal form - would generate rich response behaviour and the study of sub- and super-harmonic phenomena would probably be the most fruitful area of experimental interest. To this end, a cantilever beam which contains one single-side edge fatigue crack (Fig. 1a) has been subjected to a sinusoidal excitation at its free end.

Cracked beam finite elements, being one-dimensional, cannot model the stress field near the crack tip; thus, a frictionless contact model for a breathing crack with two-dimensional finite elements is used here which avoids computing the stress intensity factors separately. It should be mentioned that a frictionless contact model for a breathing crack is used, and a non propagating crack assumption is made in the following discussion; in other words, it is assumed that in the present loading history the crack remains stable and does not grow further.

Analyses are carried out in both time and frequency domains, for a given position and depth of the crack; the forcing frequency has been assumed as a parameter and its influence on the steady state response of the cracked beam has been systematically studied within a broad range with respect to the first natural frequency of the system. The response is described in terms of displacement and velocity fields as well as contact forces at the crack interfaces, and have been presented in the form of Fourier spectra, phase plane portraits, bifurcation diagrams and time-histories of the relevant quantities.

In this paper, a sample application has been worked out which refers to a single crack with assigned severity and position. The authors intend to investigate the dynamic response of the beam for different values of the above mentioned parameters in a future work the goal of which will be to qualitatively and quantitatively relate the nonlinear features of the beam motion to the damage detection.

2. System model

2.1 Generalities

This problem physically represents a straight beam of length L which contains one single-side edge fatigue crack of depth a and has a rectangular uniform cross-section of height h and width b (Fig. 1a); the cantilever beam is clamped at the left end and free at the right end. The crack is located at the upper edge of the beam at a distance d from the fixed end and $p=d/L$ is the dimensionless crack position; the severity $s=a/h$ of the crack is expressed in terms of the ratio between the depth to the height of the cross-section. Linear isotropic stress-strain material properties are assumed.

The breathing crack is modelled as a contact problem between the crack interfaces: the contactor (elastic) edge on the free end side and the target (rigid) edge on the fixed end side, i.e. contact ocurs at a point between a rigid and a flexible body; the contact model will be described in the next section.

While the beam is vibrating, the state of the crack section varies from detachment to compression, i.e. the crack opens and closes with time. This results in a modification of the crack section stiffness, the extremal values being the stiffness of the open crack and that of the intact beam. Thus, the nonlinear behaviour of the closing crack introduces the characteristics of the nonlinear systems. However, for many practical applications, the system can be considered bi-linear, and the fatigue crack can be introduced in the form of the so-called "breathing crack" model which opens when the normal strain near the crack tip is positive, otherwise it closes [11]. Distinction should be made between the first natural frequencies $\omega_1=2\pi/T_1$ and $\omega_2=2\pi/T_2$, of the two constituent sub-models (open crack (1) and closed crack (2)) and the first natural frequency ω_0 of the system, the so-called *bilinear frequency* [6]:

$$\omega_0 = 4\pi/(T_1+T_2) = 2\omega_1\omega_2/(\omega_1+\omega_2) \qquad (1)$$

where T_1 and T_2 are the natural periods of the two sub-models. Equation (1) strictly holds for a single-degree-of–freedom oscillator with a bilinear stiffness; as it will be seen in Subsect. 4.1, Equation (1) approximates with good accuracy the first natural frequency of the beam with breathing crack.

Herein, the plane-stress elastodynamic response of an edge cracked panel is studied via a contact model for a breathing crack associated with two-dimensional finite element discretization [12], using the code ADINA 8.1 [13]. A 2-D solid (plane stress) nine-node isoparametric element was chosen to discretize the body and the finite element mesh consisted of 3559 degrees-of-freedom (Fig. 1b). A consistent mass matrix is used with implicit time integration, provided that the *Newmark* method and

full *Newton* iteration are used. Two-dimensional contact surfaces are specified to model planar contact behaviour between solid elements at the crack interfaces (Fig. 1d).

2.2 Contact modelling

Contact surfaces are defined as surfaces that are initially in contact or are anticipated to come into contact during the response solution. Two-dimensional contact surfaces are formed of a series of linear contact segments and each segment is bounded by two nodes, Fig. 1c. A distinction should be made within these two surfaces between the contactor surface and the target surface, in as much, in the converged solution, the target nodes can overlap the contactor body and not vice-versa; in other words, according to the contact condition, the contactor nodes cannot be inside the target body, but the target nodes can be inside or outside the contactor body. A node of the contactor surface can come into contact with a segment of the target surface.

In frictionless contact, the possible states of the contactor nodes and/or segments are: (i) the gap between the contactor node and target segment is open (no-contact); (ii) formerly closed gap has opened; a tensile force onto the contactor node is not possible (tension release); (iii) the gap between the contactor node and the target segment is closed; a compression force is acting onto the contactor node.

The finite element approach is used to discretize the governing continuum mechanics equations and the contact conditions. To exemplify the formulation of the governing finite element equations, let us consider the two-dimensional case of contactor and target bodies shown schematically in Fig. 1c, where the target segment corresponding to contactor node k is defined by nodes k_1 and k_2. The target point k_t is the closest point of the target segment k_1-k_2 to the contactor node k. By assembling for all contactor nodes the nodal point force vectors, the discretization of the continuum mechanics equations corresponding to the conditions at time $t+\Delta t$ gives [13]:

$$\mathbf{f}_i(\mathbf{u}) = \mathbf{f}_e - \mathbf{f}_c(\mathbf{u}, \boldsymbol{\lambda}) \tag{2a}$$

$$\mathbf{c}_c(\mathbf{u}, \boldsymbol{\lambda}) = \mathbf{0} \tag{2b}$$

where $\mathbf{u}$, $\boldsymbol{\lambda}$ are the solution variables, namely the nodal point displacements $\mathbf{u}$ and the normal traction components $\boldsymbol{\lambda}$; $\mathbf{f}_i$ is the vector of internal nodal forces equivalent to element stresses; $\mathbf{f}_e$ is the vector of applied external nodal forces; $\mathbf{f}_c$ is the nodal force vector, which is obtained by assembling for all con-

tactor nodes the nodal point force vectors due to contact; $\mathbf{c}_c$ is the vector of contact conditions the components of which are as many as the contactor nodes.

The incremental finite element equations of motion including contact conditions for solution of Eqs. (2) are obtained by linearization about the last calculated state at time t :

$$\begin{bmatrix} \left(\mathbf{K}_T + \mathbf{K}_{uu}^c\right) & \mathbf{K}_{u\lambda}^c \\ \mathbf{K}_{\lambda u}^c & \mathbf{K}_{\lambda\lambda}^c \end{bmatrix} \begin{Bmatrix} \Delta\mathbf{u} \\ \Delta\boldsymbol{\lambda} \end{Bmatrix} = \begin{Bmatrix} \mathbf{f}_e^{t+\Delta t} - \mathbf{f}_i - \mathbf{f}_c \\ -\mathbf{c}_c \end{Bmatrix} \tag{3}$$

where $\Delta\mathbf{u}$ and $\Delta\boldsymbol{\lambda}$ are the increments in the solution variables $\mathbf{u}$ and $\boldsymbol{\lambda}$, $\mathbf{K}_T$ is the usual tangent stiffness matrix including geometric nonlinearities, not including contact conditions; $\mathbf{K}_{uu}^c$, $\mathbf{K}_{u\lambda}^c$, $\mathbf{K}_{\lambda u}^c$, $\mathbf{K}_{\lambda\lambda}^c$ are the contact stiffness matrices. It is worth to be noticed that the vector $\mathbf{f}_e$ is evaluated at current time $t+\Delta t$, while the other matrices and vectors are evaluated at the previous time t.

In order to simplify the notation, the following relations are understood to refer to any contactor node k. Using the definition of the "gap function" g, that is the (signed) distance from the node k to the target point k_t, the conditions for normal contact can be stated as the *Signorini*'s in displacements conditions [14]:

$$g \geq 0, \tag{4a}$$

$$\lambda \geq 0, \tag{4b}$$

$$g\,\lambda = 0 \tag{4c}$$

Note that the contact force and gap function are of course expressed in terms of the nodal displacements.

Equations (4) can be interpreted by considering the following cases:

1) *no contact*: if $g>0$, the equality in Eq. (4c) implies $\lambda=0$; when there is no contact, all contact tractions must be zero;
2) *sticking contact*: if $\lambda>0$, the equality in Eq. (4c) implies $g=0$.

Accordingly, any component of the vector $\mathbf{c}_c$ which refers to any contactor node k can be written as

$$c_{cw} = \hat{w}(g,\lambda) \tag{5}$$

and the following constraint function can be used [13]:

$$\hat{w}(g,\lambda) = \frac{g+\lambda}{2} - \sqrt{\left(\frac{g-\lambda}{2}\right)^2 + \varepsilon_N} \tag{6}$$

where ε_N is very small but larger than zero. Equation (6) defines a suitable function of g and λ such that the solutions of $\hat{w}(g,\lambda)=0$ satisfy the conditions (4) within a reasonable accuracy.

2.3 Solution of nonlinear equations of motion

The solution of the nonlinear dynamic response of the finite element system at hand is obtained using the incremental formulation presented in Subsect. 2.2, an iterative solution procedure and a time integration algorithm. For notation's conciseness, the following symbols are introduced:

$$\mathbf{U}=\begin{Bmatrix}\mathbf{u}\\ \boldsymbol{\lambda}\end{Bmatrix},\ \mathbf{F}=\begin{Bmatrix}\mathbf{f}_e\\ \mathbf{0}\end{Bmatrix},\ \mathbf{R}=\begin{Bmatrix}\mathbf{f}_i+\mathbf{f}_c\\ \mathbf{c}_c\end{Bmatrix},\ \mathbf{K}=\begin{bmatrix}\left(\mathbf{K}_T+\mathbf{K}^c_{uu}\right) & \mathbf{K}^c_{u\lambda}\\ \mathbf{K}^c_{\lambda u} & \mathbf{K}^c_{\lambda\lambda}\end{bmatrix}.$$

The solution of the equilibrium at time $t+\Delta t$ requires an iteration procedure: by linearizing the response of the finite element system about the conditions at time $t+\Delta t$, iteration (i-1), the following equations are obtained:

$$\Delta\mathbf{F}^{(i-1)}=\mathbf{F}_{t+\Delta t}-\mathbf{R}^{(i-1)}_{t+\Delta t} \tag{7a}$$

$$\mathbf{K}^{(i-1)}_{t+\Delta t}\,\Delta\mathbf{U}^{(i)}=\Delta\mathbf{F}^{(i-1)} \tag{7b}$$

$$\mathbf{U}^{(i)}_{t+\Delta t}=\mathbf{U}^{(i-1)}_{t+\Delta t}+\Delta\mathbf{U}^{(i)} \tag{7c}$$

In each iteration an out-of-balance load vector is calculated, Eq. (7a) and an increment in displacements is given by Eq. (7b): this leads to update **K** and **R**. The iteration proceeds until the out-of-balance load vector $\Delta\mathbf{F}^{(i-1)}$ or the displacement increments $\Delta\mathbf{U}^{(i)}$ are sufficiently small.

Newmark's method with $\delta=1/2$ and $\alpha=1/4$ is used for time integration and the robustness of the numerical procedure has been checked in all the performed analyses.

3. Impulsive dynamics

3.1 Model data

A cracked cantilever beam (Fig. 1a) of length 300 mm and cross-section 20×20 mm^2 was tested and studied by Rizos *et al*. [15]; the material is mild steel having *Young*'s modulus 206.8 GPa, *Poisson* ratio 0.3, and mass density 7850 kg/m^3. The vibration frequencies and mode shapes of the same linear beam containing an open edge-crack of various sizes at different positions along the beam were experimentally obtained by Kam and Lee [16] while a finite element analyses has been performed in [17].

3.2 Impulsive loading

Free vibrations of the cracked beam after impulsive excitation have been numerically analysed under instantaneous loading. An impulsive force of 2 KN has been transversally applied for a very short while ($\Delta t \cong 0.02\ T_0$) at the end of the cracked beam (Fig. 1a) and the amplitude of the end transverse displacement has been recorded as soon as a steady state has been attained. It has been assumed that the forced system reaches its steady state when the maximum displacement amplitude of the transient response varies to an extent less than 0.1%. The frequency content of the y-displacement time-history of the loaded point has been determined via spectral analysis in order to evaluate the lowest three natural frequencies of the beam with breathing crack. It is worth noting that the vibration amplitude does not affect the natural frequencies due to the bilinear character of the nonlinearity of the problem at hand [18]; as a consequence the magnitude of the applied load does not affect the frequency content and the relative importance of the harmonic components of the system response, that is confirmed by numerical tests performed via finite element 2D model of cracked beam.

Filled contour maps of Fig. 2 [19] pictorially and simultaneously illustrate the combined influence of crack position and severity on the lowest three natural frequencies of the cracked beam. The two dimensions of each rectangular domain are the length of the beam and the largest crack depth (a=0.75h). Fill attributes are assigned so that there is a gradation change of colour from the minimum to maximum contours. Moreover, a colour scale shows the fill assigned to each colour on a filled contour map and the numerical value for each level are displayed. The values measure (in percentage) the difference between the frequencies f_u of the uncracked beam and the reduced frequencies f_c of the cracked beam, with respect to the former value f_u, i.e. $(f_u\text{-}f_c)/f_u$%. For given position and severity of the crack, the frequency reduction can be estimated on the contour map. As can be seen, the effect of position and severity of the crack in the three modes is quite different. The reduced frequencies are, as expected, intermediate between open crack and intact beam [19].

4. Harmonically forced Response

4.1 Generalities

The following non-dimensional parameters are found to be significant: (i) the severity of the crack $s=a/h$ depth-to-height ratio, (ii) the position of the crack $p=d/l$ distance-to-length ratio, and the excitation-to-system frequency ratio, $\eta=\Omega/\omega_0$, where Ω is the frequency of the harmonic excitation and ω_0 is the first natural frequency of the system.

The cantilever response depends on the above listed parameters. A detailed features of the response is studied for a damage scenario characterized by a severity factor $s = 0.5$, a position factor $p = 0.27$ (see Fig. 1a), while the driven frequency η is step-varied in the range 0.1-1 and only $\eta=2$ is considered above 1. For this damage, the analysis conducted in [19] allows the following values to be found out: ω_1=160 Hz for the open crack beam, ω_2=183.3 Hz for the uncracked beam, and ω_0=170 Hz for the breathing crack beam, which coincides with the value given by Eq. (1). The amplitude $A = 0.4$ KN is considered for the sinusoidal load applied at the beam tip. The time step taken is about (1/60) times the time-period $2\pi/\omega_0$, i.e. 0.0001 s. The Discrete Fourier Transform (DFT) is used to perform spectral analysis of the dynamic response.

For different values of η, the Fourier spectra of the displacement time-histories of the load point (FSR) have been depicted in Fig. 3, in the form of 2-D histograms. The frequency content is reported in terms of Ω, and its integer multiples (n) and sub-multiples ($1/n$). Whatever the driving frequency, the response fundamental component Ω, i.e. n=1, attains the largest amplitude in all the cases but $\Omega = \omega_0/2$ and $\Omega = 2\omega_0$; furthermore, the exhibited behaviour is quite complex, characterized by even and odd super- and sub-harmonic frequencies, and non-integer multiples depending on the forcing frequency. The amplitude of the other components is evaluated in percentage with respect to the amplitude of the fundamental component, and has been discarded when smaller than 1%.

4.2 Detailed description

The forced response of the cracked beam has been investigated for different value of η; herein, only the most characterising results of the performed analysis have been reported, namely η = 1/4, 1/3, 1/2, 1, 2, and more few cases slightly shifted with respect to the above mentioned values of η are studied to test the robustness of some phenomena.

As far as η = 1/4 is concerned (Fig. 3a), the forced response has even and odd components at frequencies 2, 3, 4, 5 and 6Ω; the exact coincidences ω_0-Ω=3Ω, ω_0+Ω=5Ω and ω_0+2Ω=6Ω deserve to be emphasized, as already observed in [6]. The amplitude of FSR gets its maximum – if the funda-

mental component is excluded - at the fourth harmonic, which coincides with the system bilinear frequency (ω_0=4Ω); this harmonic gets here its absolute maximum, 70% of the Ω-component, throughout the whole range considered for η, as can be seen in Fig. 5a, where the amplitudes of the 2nd, 3rd, and 4th at the different driven frequencies are reported.

For a value of $\eta \cong 2/7$ slightly larger than 1/4, Fig. 3b, the expected sub-harmonic ω_0 -3Ω , which in this case coincides with Ω/2, leads to a period doubling. The response is characterized by a high number of super-harmonics; in particular the harmonic (7/2)$\Omega \cong \omega_0$ gets the largest amplitude, except the fundamental harmonic.

When η = 1/3, Fig. 3c, the forced response has small even components and one expected important odd component at 3Ω=ω_0, which coincides with the system frequency; moreover, this harmonic gets here its absolute maximum throughout the whole frequency range and is comparable to the fundamental component. In the phase plane of the load point P_2 (Fig. 1b), two wiggles appear (Fig. 4a) due to rebounding during the contact phase. For a value η = 0.327 close but different of 1/3, the wiggles disappear as the contact comprises only one expansion-compression phase; the phase plane portrait is characterized by a "figure-of-eight" shape, Fig. 4b, due to the fact that the component 3Ω is just outside the narrow super-harmonic resonance range and is much less important.

At η =1/2, Figs. 3d and 4c, the forced response has two even components at frequency 2Ω=ω_0 and 4Ω = 2ω_0. It should be pointed out that the 2nd harmonic gets its maximum amplitude (Fig. 5a), and is even larger than the fundamental one $\Omega = \omega_0/2$.

The coincidence of the harmonic ω_0 - Ω with the sub-harmonic Ω/2 at half the driving frequency should be noted (Fig. 3e) for η = 2/3. The phase plane portrait of the load point P_2 (Fig. 1b) is plotted in Fig. 6a, where the y-trajectory of the load point has been sampled at the driving frequency and the two clusters of points of the relevant *Poincaré* sections are evidenced. As already observed in experimental studies [20], the period-two (Ω/2) sub-harmonic (Fig. 3e) is associated with a bifurcation, as shown in Fig. 6b, where the frequency-amplitude pairs have been reported, with reference to the y-displacement of point P_2. Analogously, Figure 6c shows two cycles of forcing which correspond to one cycle of response. It is worth noticing that this period doubling persists only within a small range $\eta \in$[0.6454, 0.6781]. For the other values of η up to resonance, the forced response has only one small even component at frequency 2Ω, and all the response plots in the phase plane become similar ovals.

Finally, the frequency $\eta = 2$ (Fig. 3f) induces a forced response which has the fundamental component at frequency $\Omega = 2\omega_0$, and exhibits a prevailing sub-harmonic $\Omega/2 = \omega_0$ at half the driving frequency, which paramountly overcomes the fundamental one, the phase portrait tending to an oval with a very small wiggle (Fig. 4d) representative of the small driving component Ω.

Generally speaking, the importance of the harmonics on the frequency axis change with a change in exciting frequency as illustrated by Figs. 5a and 5b; the 3-D histograms report the amplitude of the harmonics in terms of η and the multiples and sub-multiples of the driving frequency Ω. The amplitude of any harmonic increases in the vicinity of the bilinear frequency ω_0, and then it gradually decreases away from ω_0. Thus, it can be stated that if the forcing frequency is such that any one of its multiples (n=2,3,4,…) and sub-multiples (n=1/2,1/3,1/4,…) is close to the first natural frequency of the system, then that order of the harmonic will have a high amplitude in spite of the fact that the amplitudes of the higher harmonics are usually small.

It is noteworthy that the 3rd component is strong enough also at $\omega_0 + \Omega = 3\Omega$ (Fig. 3d), i.e. for an excitation at $\eta = 1/2$; in this case the neighbouring 2nd harmonic, being very close to the system frequency, is very large and hence it strongly influences the 3rd harmonic in spite of the latter being further away from the system natural frequency.

Finally, it can be observed that the periodicities of the composite model extinguish those of the alternating constituents; in other words, the steady state response is characterized by ω_0, Ω and by other minor components, which are exactly $(2n\text{-}1)\Omega$ away (n =…-2,-1,0,1,2,…) from ω_0, as predicted by the closed-form solution [6].

4.4 Impulsive behaviour of crack closing

For the lower frequencies in the range $\eta \in$ [0.123, 0.288], evidence of multiple impacts emerges. They become clear in the phase plane portraits of relative velocity versus relative displacement (relative phase plane) in the z direction at the upper edge of the crack interfaces. Typically the faces of the crack will have nonzero relative velocity on closure, leading to an impact. The relative phase plane portrait at the crack interfaces in z direction for the response to η=1/2 is shown in Fig. 7 to illustrate the phenomenon. This figure shows a sharp change in relative velocity, whilst relative displacement at the origin is almost unchanged. Such very steep portions of the plot are revealing of a “quasi-impulsive” behaviour. In the vicinity of the origin there is an emphatic impulsive event; the relative displacement at

the crack interface, the relative velocity and the contact force are respectively drawn in Figs. 8a,b,c for two impulsive events. The contactor body rebounds against the target body without loosing contact, i.e. detachment is almost grazed during the compressive half-cycle (Fig. 8c); this behaviour is reflected by the "wiggle" exhibited in the *y*-direction phase plane of the tip response (Fig. 4c). The $\eta = 2/7$ excitation too shows the strongest evidence of multiple impacts within the periodic trajectory, illustrated in Figs. 8d,e,f. Figures 8c,f could explain the meaning of the term "quasi-impulsive": the contact model of the crack allows for full detachment and closure under elastic response of the contacting interfaces; the very short duration of the contact phase and the very large values of the contact forces exchanged during this phase strongly resemble an impact event and therefore an impulsive-like behaviour may be recognized in the cracked beam response.

The complexity of the above mentioned behaviour during contact had been already pointed out as far as SDOF oscillators with hysteretic motion-limiting stop were concerned [21]: the time range between the contact phases got shorter until the contact duration were so long that the mass oscillated when attached to the stop; simultaneously the responses showed repeated reversals where several subsequent compression and expansion paths alternated during the same contact phase. Furthermore, an analogous phenomenon could be observed in the stick-slip vibrations of friction oscillators [22,23] with short interruptions of the stick mode being possible; pushed by spring forces the mass slowed down with respect to the moving belt, while re-entering the stick mode after a small wiggle.

4.6 One degree of freedom system

As already observed, one can qualitatively see that the global stiffness of the cracked beam depends on whether the crack is open or closed. Moreover, due to boundary conditions, loading type and crack location the first mode of the cracked beam's response is primarily involved, that can be reasonably studied by a simple system with bilinear stiffness.

In the past [6,24,25] and more recently Chati, Rand and Mukherjee [26] modelled the cracked beam as a bilinear single degree of freedom system (Fig. 9). The system consists of a lumped mass m which makes contact with the linear spring k_1 when $x<0$ and with the linear spring $k_2 > k_1$ when $x>0$. The equations of motion for the system are

$$m\ddot{x} + k_i x = 0 \text{ , } i=1 \text{ for for } x<0 \text{ and } i=2 \text{ for } x>0 \tag{8}$$

where the dot indicates differentiation with respect to time. The effective natural frequency ω_0 of this bilinear single degree of freedom system (BSDOF) is given by Eq. (1).

Identifying the BSDOF properties on the basis of the beam characteristics leads to the following values (see Subsect. 4.1): $\omega_1 = 160.0$ Hz (open crack), $\omega_2 = 183.3$ Hz (closed crack), $\omega_0 = 170.0$ Hz (breathing crack), $k_2 = 1.0$, $m = k_2/(\omega_2)^2$, $k_1 = m(\omega_1)^2$, $k_0 = m(\omega_0)^2$, $F = k_0 x_{st} \cong k_0(x_{st}^c - x_{st}^o)/2$ (the apices "o" and "c" mean "open crack" and "closed crack" respectively); the symbols $x_{st}^o<0$, $x_{st}^c>0$ refer to the deflections of the beam tip loaded by a statically applied force with the same amplitude of the sinusoidal excitation; in the first case the force downloads to open the crack, whereas in the second case it uploads to close the crack (Fig. 1a); x_{st} is the equivalent static displacement of the BSDOF.

The steady state forced response of the BSDOF has been analyzed and the phase plane portraits have been depicted for η=0.284, 0.327, 0.654, and 2. By comparing thin red curves (BSDOF responses) with thick blue curves (cracked beam responses) in Fig. 10, a good agreement between the corresponding phase plots relevant to the cracked beam and to BSDOF is found.

The effectiveness of the BSDOF oscillator which is somehow equivalent to the breathing crack beam can be useful firstly to explore a wide range of problem parameters with low computational efforts, then to capture interesting features of the dynamic response in order to investigate in more detail these findings by means of the more complex tool of the 2D FE model, which accounts for intermediate stages of crack closing and local effects of contacting surfaces and the contribution of higher modes.

5. Conclusions

The main effort of this paper has been devoted to the characterization of the nonlinear response of a cantilever cracked beam to a harmonic loading, adopting a 2D finite element formulation, which is capable to simulate the behaviour of a breathing crack via a frictionless contact model of the interacting surfaces. To this aim a systematic investigation has been performed assuming the driving frequency as a control parameter. The results of the analyses allowed to find out some interesting phenomena that characterize the nonlinear features of the motion of the cracked beam.

The presence of an unsymmetrical breathing crack in the beam makes the system strongly nonlinear with unsymmetrical restoring force characteristics, resulting in bilinear stiffness. In addition,

because of the peculiar nonlinearity, the frequency does not change with the oscillation amplitude, whilst the steady state response is very rich of sub- and super harmonic components. In this connection when the forcing frequency coincides with or is close to any one of the integer sub-multiples ($1/n$) of the first system frequency ω_0, then the nth harmonic component of the forcing frequency, which is close to ω_0, will be significantly exalted. Moreover, within the super-harmonic resonance ranges, in the cases η =1/4, 2/7, 1/3, 1/2 the phase plane portraits are characterized by significant wiggles due to impacts between the crack edges.

Furthermore, whenever the forcing frequency Ω is much smaller than both the natural frequencies of the sub-systems, minor components appear exactly $(2n\text{-}1)\Omega$ away from the major components at ω_0, as predicted by the closed-form solution for a bilinear oscillator [6], and the response exhibits bifurcation phenomena. In the case studied, a period doubling arises in small windows in the range of η <1, namely in the neighbours of η = 2/7, η = 2/3, and η = 2; in the latter case, the response shows a sub-harmonic component, $\Omega/2=\omega_0$, which very largely prevails on the fundamental $\Omega = 2\omega_0$.

In a large range of low frequency a "quasi-impulsive" event is revealed by sharp changes in the relative velocity between the crack interfaces on closure; this behaviour produces a rich variety of super-harmonics and hence "wiggles" in the phase plane plots, which can be related to repeated "impacts" without detachment, as for η = 1/2 .

Finally, since the cracked beam excited in the region of primary resonance mainly vibrates in its first mode, it is shown that an equivalent bilinear oscillator strongly resembles, at least in the examined cases, some of the fundamental aspects of the periodic response, namely the frequency content of the response, without exhausting the variety of the beam motions. So, it seems reasonable to get information about the more complex response of the cracked beam via the much simpler bilinear single-degree-of-freedom system; in particular, easily and fast analysing the response of the BSDOF within wide ranges of driving frequencies could guide the research towards the richer features of the cracked beam. In particular the beam model retains information on the crack location, that is fundamental in the damage detection.

The main features of the cracked beam response have been here highlighted; in particular when the excitation frequency is approximately $1/n$ or n of the first system frequency, the amplitude of the $(1/n)^{th}$ or n^{th} harmonic becomes appreciably large and hence detectable; then, a future study of their depend-

ence on position and severity of the crack should open interesting perspectives towards sub- and super-resonant diagnostics for detection of a breathing crack in a beam.

ACKNOWLEDGEMENTS

This research was partially funded by the Italian Ministry of Education, University and Research (MIUR) by means of the PRIN 2003 (2003080575) and by the University of Rome "La Sapienza" by means of the Progetto di Ricerca di Ateneo 2003 (C26A038198). Moreover, the authors whish to thank Pier Mario Pollina, Ph.D student in Theoretical and Applied Mechanics (University of Rome), who worked out computer simulations.

References

[1] Doebling, S.W. and Ferrar, C.R. and Prime M.B., 1998, "A summary review of vibration based damage identification methods," Shock and Vibration Digest **30**, 91-105.

[2] Vestroni, F., and Capecchi, D., 2000, "Detection of Damage in Beam Structures Based on Measurements of Natural Frequencies", J. of Engineering Mechanics, ASCE, **126**(7), pp. 761-768.

[3] Chondros T.G. and Dimaronogas A.D., 'Vibration of a cracked cantilever beam', *Transaction of the ASME*, **120**, 742-746, 1998.

[4] Chondros, T. G., Dimarogonas, A. D., and Yao, J., 2001, "Vibration of a Beam with a Breathing Crack", J. of Sound and Vibration, **239**(1), pp. 57-67.

[5] Cheng, S. M., Wu, X. J., and Wallace W., 1999, "Vibrational Response of a Beam with a Breathing Crack", J. of Sound and Vibration, **225**(1), pp. 201-208.

[6] Chu, Y. C., and Shen, M.-H. H., 1992, "Analysis of Forced Bilinear Oscillators and the Application to Cracked Beam Dynamics", AIAA Journal, **30**(10), pp. 2512-2519.

[7] Tsyfansky, S. L., and Beresnevich, V. I., 2000, "Nonlinear Vibration Method for Detection of Fatigue Cracks in Aircraft Wings", J. of Sound and Vibration, **236**(1), pp. 49-60.

[8] Abraham, O. N. L., and Brandon, J. A., 1995, "The Modelling of the Opening and Closing of a Crack", ASME J. of Vibration, Acoustics, Stress and Reliability in Design, **117**, pp. 370-377.

[9] Ruotolo, R., Surace, C., Crespo, P. and Storer, D., 1996, "Harmonic Analysis of the Vibrations of a Cantilevered Beam with a Closing Crack", Computers & Structures, **61**(6), pp. 1057-1074.

[10] Kisa, M., and Brandon J. A., 2000, "The Effects of Closure of Cracks on the Dynamics of a Cracker Cantilever Beam", J. of Sound and Vibration, **238**(1), pp. 1-18.

[11] Dimaronogas, A. D., and Papadopolous, C. A., 1983, "Vibration of Cracked Shafts in Bending", J. of Sound and Vibration, **91**(4), pp. 583-593.

[12] Nandi, A., and Neogy, S., 2002, "Modelling of a Beam with a Breathing Edge Crack and Some Observations for Crack Detection", J. of Vibration and Control, **8**(5), pp. 673-693.

[13] Bathe, K. J., 1996, Finite Element Procedures, Prentice Hall, Upper Saddle River, New Jersey.

[14] Signorini, A., 1951, Mathematical Physics (in Italian), E.V. Veschi, Rome, Italy.

[15] Rizos, P. F., Aspragathos, N., and Dimarogonas, A. D, 1990, "Identification of Crack Location and Magnitude in a Cantilever Beam from the Vibration Modes', J. of Sound and Vibration, **138**(3), pp. 381-388.

[16] Kam, T. Y., and Lee, T. Y., 1992, "Detection of Cracks in Structures Using Modal Test Data", Eng. Fract. Mech., **42**(2), pp. 381-387.

[17] Qian, G.-L., Gu, S.-N., and Jiang, J.-S., 1990, "The Dynamic Behaviour and Crack Detection of a Beam with a Crack", J. of Sound and Vibration, **138**(2), pp. 233-243.

[18] Zuo, L., and Currier, A., 1994, "Non-linear and complex modes of conewise linear systems", J. of Sound and Vibration, **174**, pp. 289-313.

[19] Andreaus, U., Casini P., and Vestroni F., 2003, "Frequency Reduction in Elastic Beams due to a Stable Crack: Numerical Results Compared with Measured Test Data", Engineering Transactions **51**(1), pp. 1-16.

[20] Brandon, J. A., Benoit, E., and Jezequel L., 1998a, "Subtle Bifurcation in the Vibration of a System with an Interface Nonlinearity", Chaos, Solitons & Fractals, **9**(3), pp. 393-400.

[21] Andreaus, U., and Casini, P., 2000, "Dynamics of SDOF Oscillators with Hysteretic Motion-Limiting Stop", Nonlinear Dynamics, **22**(2), pp. 155-174.

[22] Andreaus, U., and Casini, P., 2001, "Dynamics of Friction Oscillators Excited by a Moving Base and/or Driving Force", J. of Sound and Vibration, **245**(4), pp. 685-699.

[23] Popp, K., Hinrichs, N., and Oestreich, N., 1996, "Analysis of a Self Excited Friction Oscillator with External Excitation", Dynamics with Friction: Modelling, Analysis and Experiment, pp. 1-35, A. Guran *et al*. eds., Series on Stability, Vibration and Control of Systems Series B, **7**, World Scientific Publishing Company, Singapore.

[24] Frisweel, N. I., and Penny, J. E. T., (1992), "A simple nonlinear model of a cracked beam", Proc. 10th Int. Modal Analysis Conf., San Diego, Ca., pp. 516-521.

[25] Shen, M.-H., and Chu, Y. C., 1992, "Vibrations of Beams with a Fatigue Crack", Computers and Structures **45**(1), pp. 79-93.

[26] Chati, M., Rand, R. H., and Mukherjee, S., 1997, "Modal Analysis of a Cracked Beam", J. of Sound and Vibration, **207**(2), pp. 249-270.

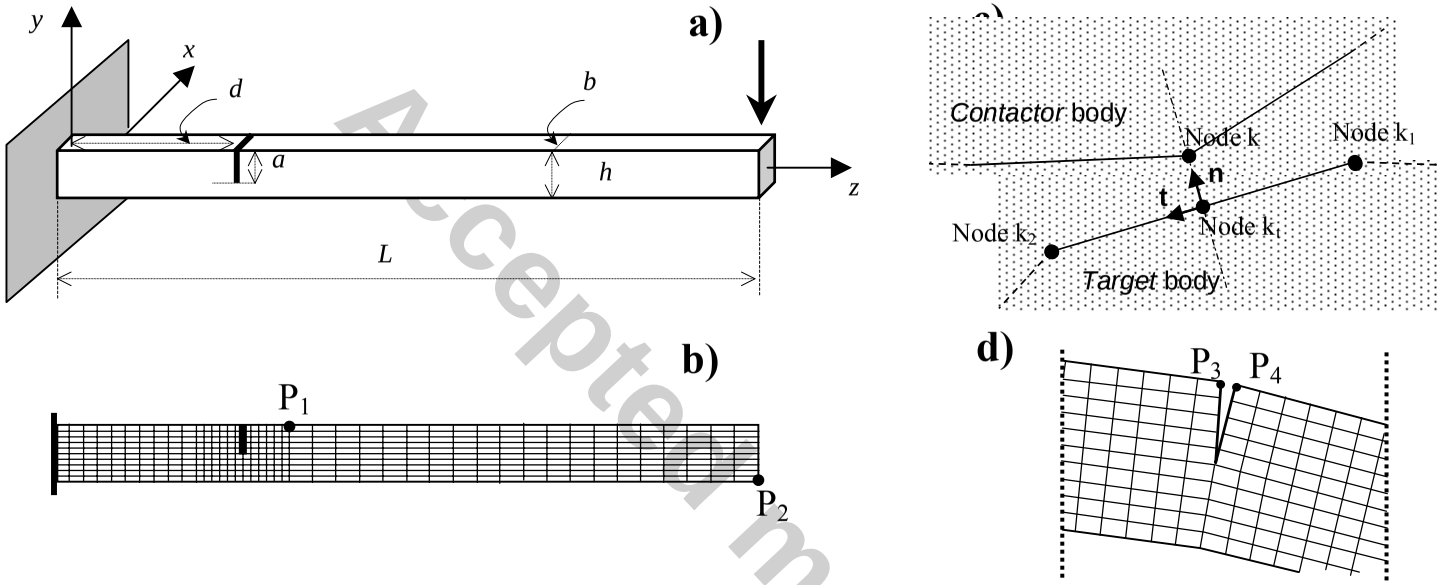

Fig. 1

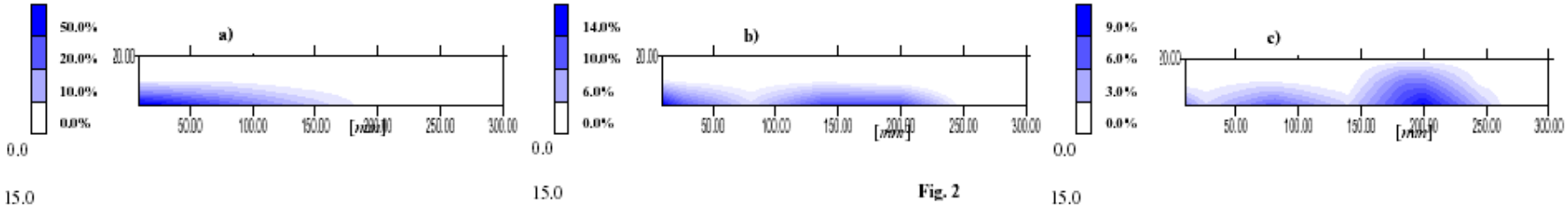

Fig. 2

Fig. 2

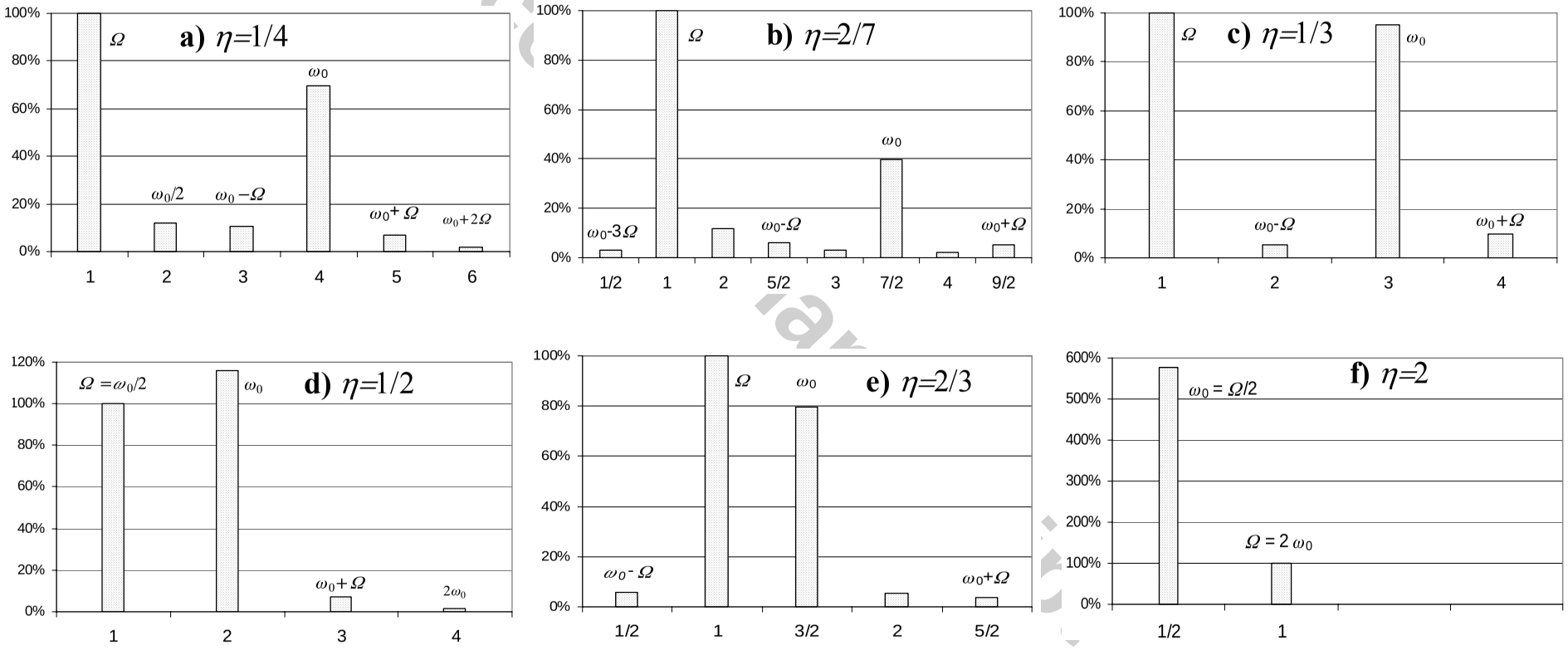

Fig. 3

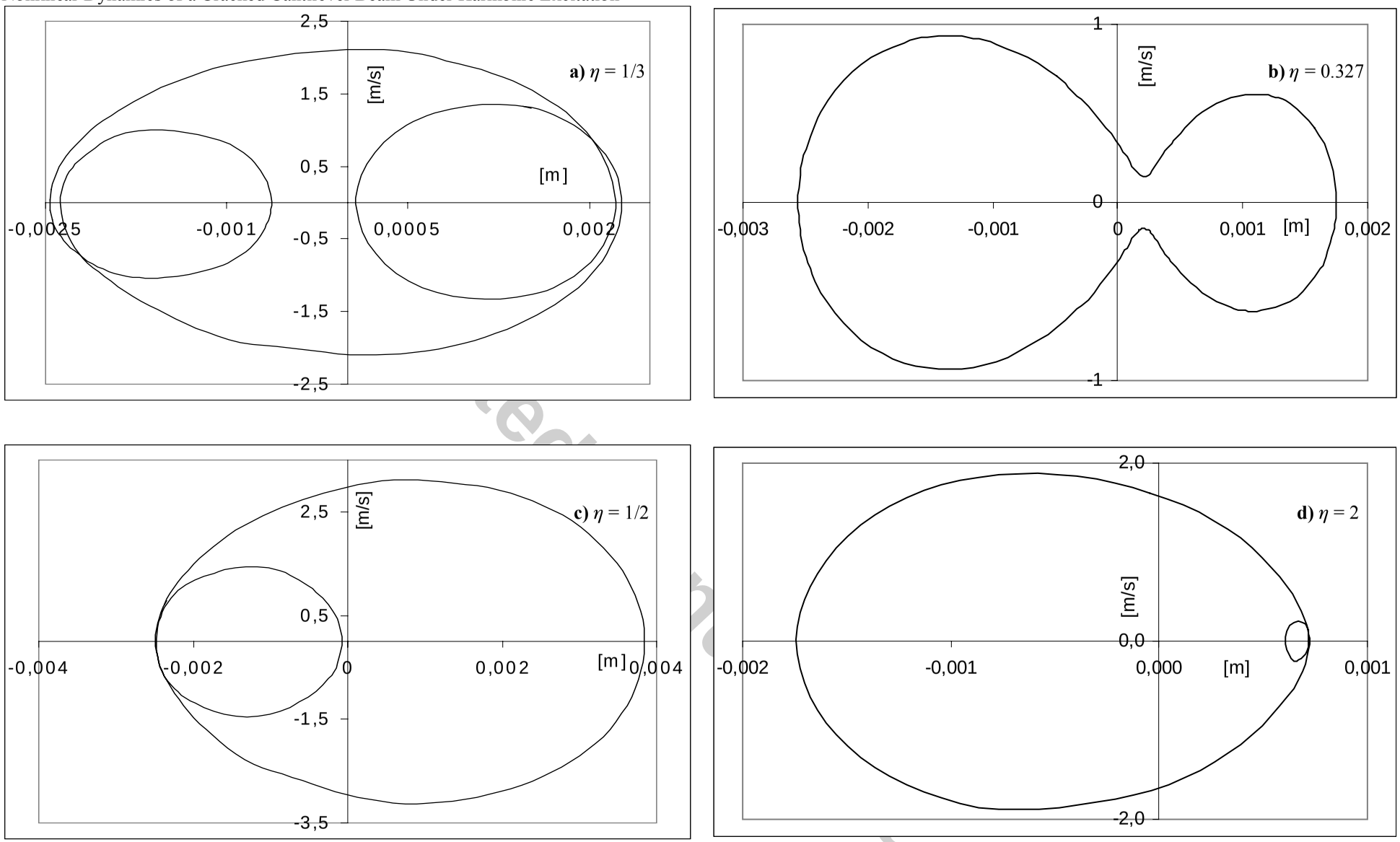

Fig. 4

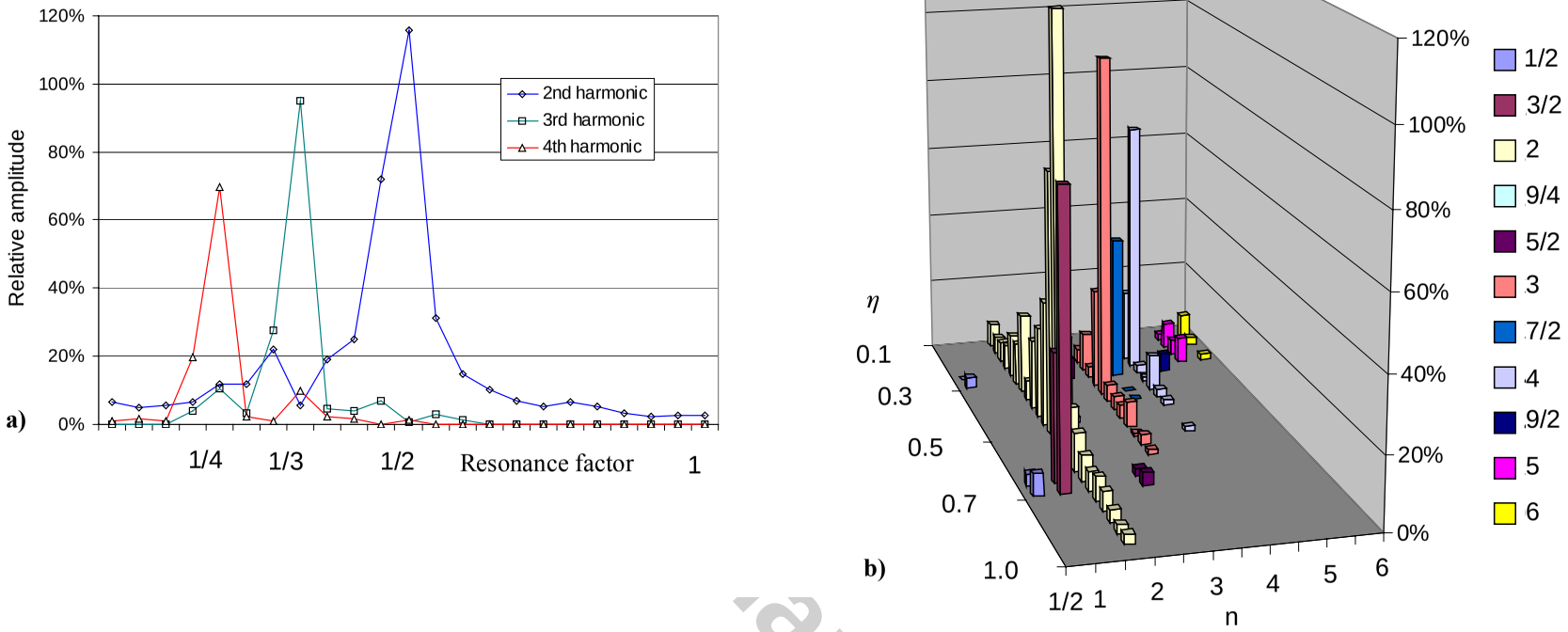

Fig. 5

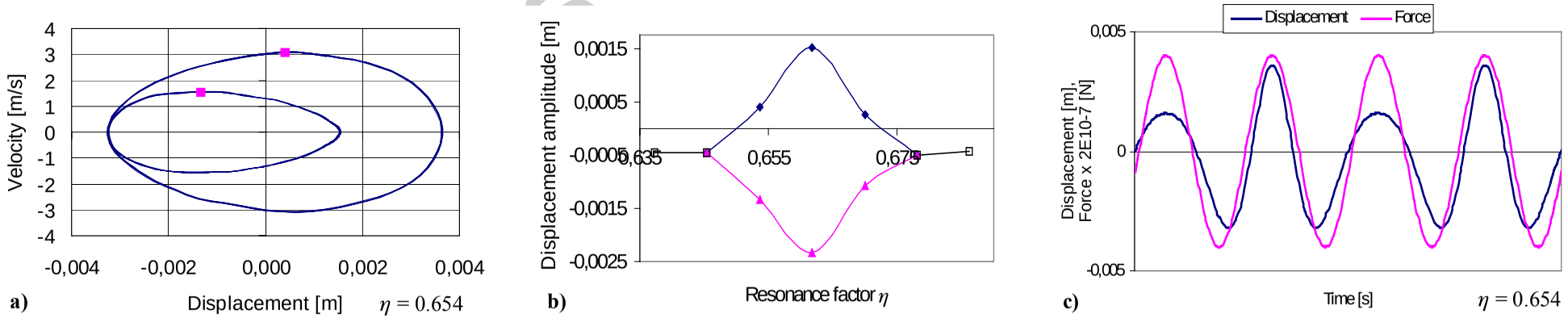

Fig. 6

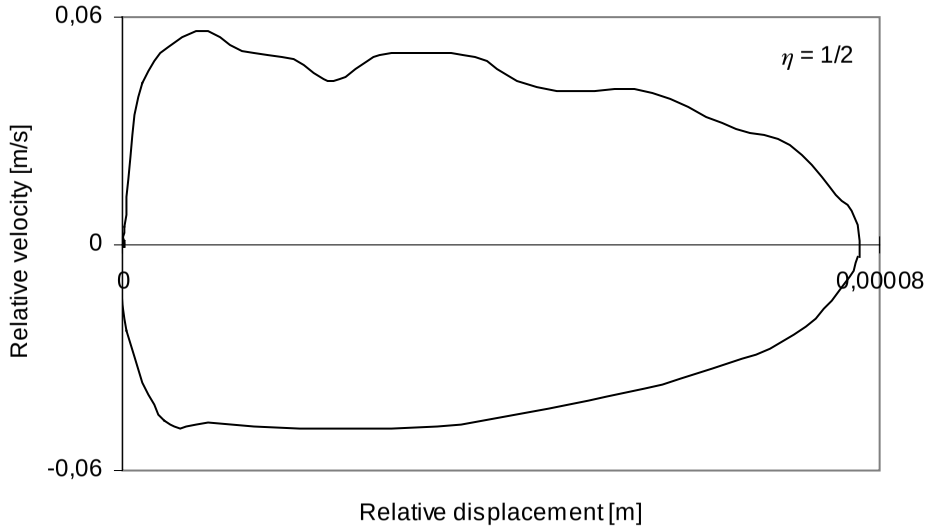

Fig. 7

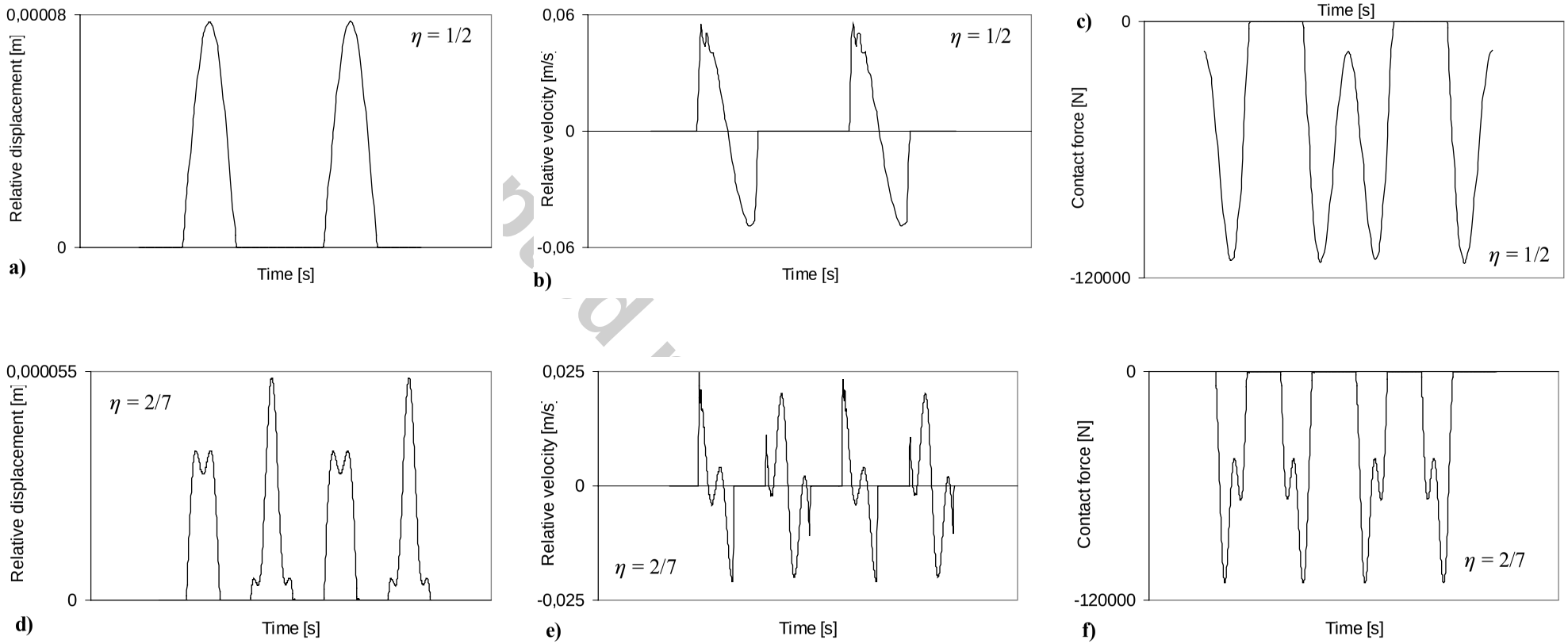

Fig. 8

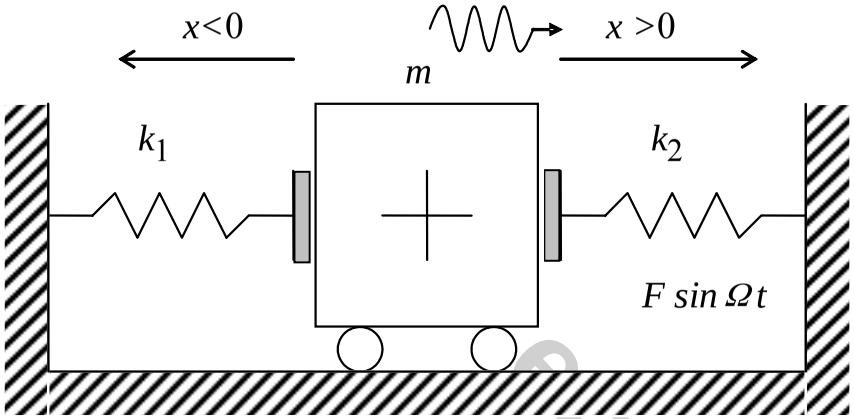

Fig. 9

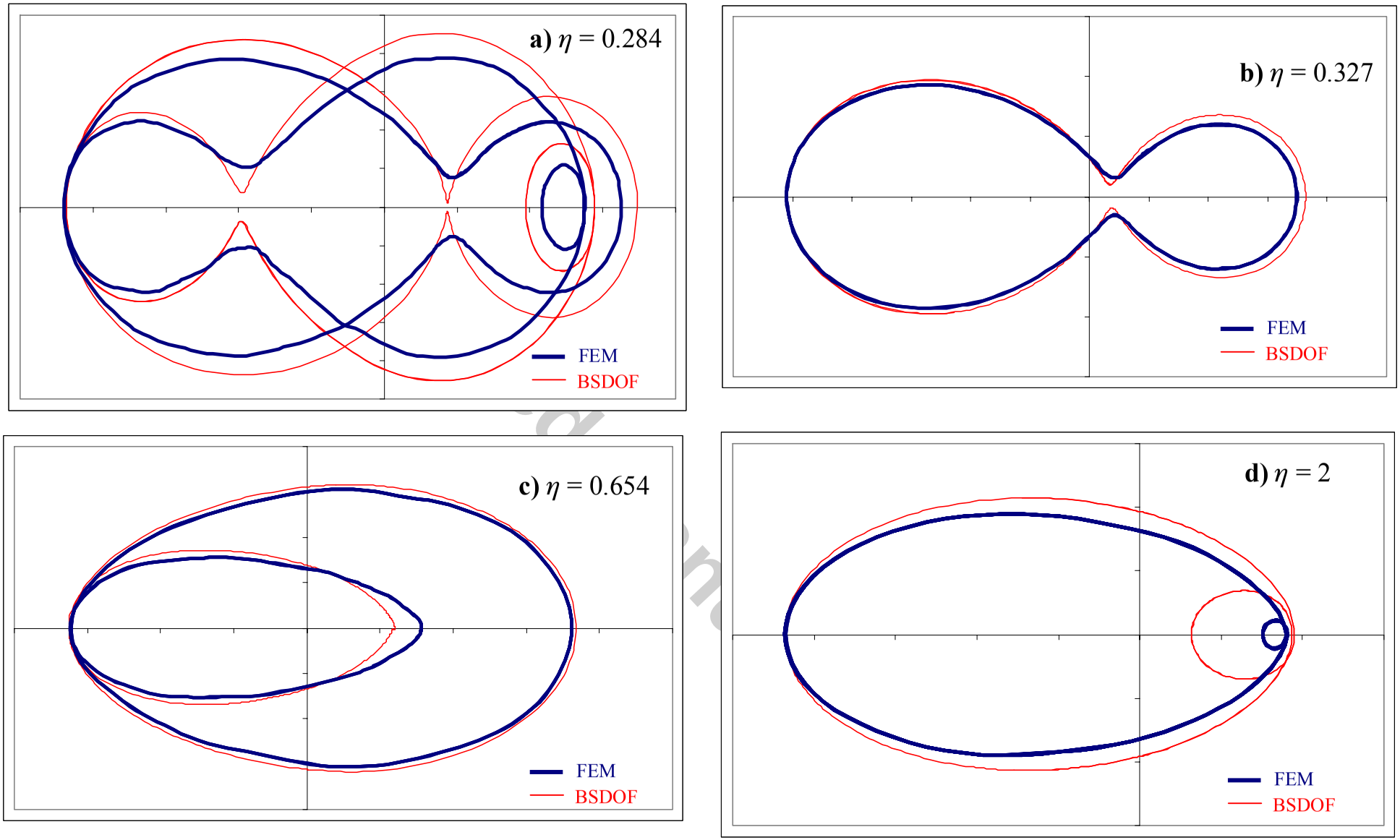

Fig. 10

Figure captions

Fig. 1 - Cantilever beam. a) Three-dimensional model; b) Finite element mesh and zoom of the cracked zone; c) Two-dimensional case of contact; d) mesh zoom of the crack zone.
Fig. 2 – Instantaneous loading. a) 1st natural frequency; b) 2nd natural frequency; c) 3rd natural frequency.
Fig. 3 –Fourier Spectra Peaks. a) $\eta = 1/4$; b) $\eta = 2/7$; c) $\eta = 1/3$; d) $\eta = 1/2$; e) $\eta = 2/3$; f) $\eta = 2$.
Fig. 4 - Absolute plane phase portraits. a) $\eta = 1/3$; b) $\eta = 0.327$; c) $\eta = 1/2$; d) $\eta = 2$.
Fig. 5 – Sub- and superharmonic frequencies (Fourier spectrum of displacement of the load point; $s = 0.5$, $p = 0.27$). a) 2-D diagram; b) 3-D diagram.
Fig. 6 – Period doubling at $\eta = 2/3$ (y-displacement of the load point): a) Poincaré section; b) bifurcation diagram $\eta \in [0.6454, 0.6781]$; c) comparison of sinusoidal load trace and displacement time history.
Fig. 7 – Relative phase plane between crack interfaces for $\eta = 1/2$.
Fig. 8 - Quasi-impulsive behaviour (time-history) at crack interfaces: $\eta = 1/2$ (a,b,c) and $\eta = 2/7$ (d,e,f). a),d) Relative displacement; b),e) relative velocity; c),f) contact force.
Fig. 9 – Single-degree-of-freedom system with bilinear stiffness.
Fig. 10 – Plane phase portrait for different η. Thick blue line: FEM of cracked beam; thin red line: BSDOF.